Homogeneous linewidths of single rotational lines in the "channel three" region of C_6H_6

E. Riedle and H. J. Neusser
Institut für Physikalische und Theoretische Chemie, Technische Universität München, D 8046 Garching, Germany

(Received 19 October 1983; accepted 6 December 1983)

Homogeneous linewidths of single rotational lines have been measured in the "channel three" region of C_6H_6. The necessary spectral resolution of about 5 MHz and the high sensitivity were achieved by Doppler-free two-photon spectroscopy within an external cavity setup. Linewidths produced by intramolecular relaxation were found to increase strongly with increasing J for $K = 0$ and constant vibrational energy $E_{excess} = 3412\ cm^{-1}$. This result together with the investigated structure in the highly resolved spectrum of the $14_0^1 1_0^2$ band is a strong indication that Coriolis coupling plays an important role in the intramolecular vibrational redistribution process.

I. INTRODUCTION

One of the fundamental problems in the spectroscopy and the understanding of the dynamics of polyatomic organic molecules is the onset of channel three in benzene. It now turns out that some of its features are typical for polyatomic molecules rather than restricted to the molecule benzene. Therefore it is expected to yield insight into the nature of primary photophysical processes within polyatomic molecules as a whole. For an excess energy of 3000 cm^{-1} in S_1 there has been found a sudden decrease in fluorescence quantum yield[1] together with a diffuseness of the absorption[2] spectrum both pointing to the onset of a fast nonradiative process. To present date, the one-photon high resolution linewidth measurements have been limited in resolution due to the Doppler broadening of the lines (1.7 GHz).[2,3] On the other hand, two-photon experiments in a supersonic jet performed by Aron *et al.*[4] have been limited by the frequency width of the laser and have been restricted to the lowest J, K lines of the spectrum due to the cooling characteristics of the supersonic jet. As a consequence of the low spectral resolution, in these experiments, a broadening of the lines is only observed if the unknown process is already so fast that any specific characteristics of the process, e.g., dependence on the J, K rotational quantum numbers of the excited rovibronic states necessary for its identification, is smeared out.

In our recent work[5] in a Doppler-free two-photon experiment, we increased the spectral resolution by nearly one order of magnitude to the 200 MHz range. This resolution together with the necessary sensitivity was achieved with a particular pulsed amplifier set up for a single-mode cw dye laser with Fourier-transform limited bandwidth. With this experimental setup we were able to measure rotationally resolved spectra just at the onset of channel three where broadening is expected to be still small enough to allow for the observation of separated rotational lines. In this spectral range we found strong indications for a rotationally dependent nonradiative process: At the blue edge of the Q branch ($\Delta K = 0$, $\Delta J = 0$) of the $14_0^1 1_0^2$ band only rotational lines with $K = 0$ are observed whereas the many other lines with $K \neq 0$ have disappeared in the two-photon excitation spectrum. From this result we concluded that Coriolis coupling is responsible for the disappearance of the $K \neq 0$ lines. The decreasing intensity of the remaining lines ($K = 0$) with increasing J points to an increasing nonradiative rate. In this spectrum, however, we did not find a remarkable broadening of the remaining lines within the experimental resolution of 200 MHz. A theoretical description of the observed spectral results has been given in our recent work.[6]

In this work quantitative information about the nonradiative behavior of an electronically excited polyatomic molecule is obtained for the first time from Doppler-free measurements of single rovibronic transition linewidths under near collision-free conditions at room temperature. Room temperature turns out to be necessary since it will be shown that the dynamic behavior of high J levels provides for the key information about the nature of the photophysical process. The homogeneous linewidths of the $K = 0$ lines in the $14_0^1 1_0^1$ and the $14_0^1 1_0^2$ band will be investigated in order to obtain quantitative information about the dependence of the nonradiative process not only on the vibrational excess energy but also on the rotational quantum numbers of the molecules. These measurements have become feasible by an external cavity setup for the Doppler-free two-photon absorption experiments which led to a substantial increase in signal strength.[7]

II. EXPERIMENTAL SET UP

The scheme of the experimental setup is shown in Fig. 1. The high spectral resolution is provided by a cw ring laser system (Coherent 699) with a linewidth of 1 MHz operating with Coumarin 102 dye and pumped by the violet lines of a Kr^+ ion laser (CR 3000 KUV). The maximum output power around 4820 Å is 400 mW. A Faraday rotator is used for decoupling of the Doppler-free two-photon experiment with counterpropagating light beams from the single-mode dye laser. In this way feedback is avoided which would lead to an uncontrolled mode hop of the laser. The linearity of the laser scan is permanently controlled with a temperature-stabilized confocal etalon with 1.5 GHz free spectral range and the wavelength of the laser light is measured with a wavemeter (Burleigh WA 20). In order to improve the signal to noise ratio in our experiments at low pressures and to increase the accuracy of the linewidth measurements the Doppler-free two-photon experiments have been performed

 0021-9606/84/104686-08$02.10

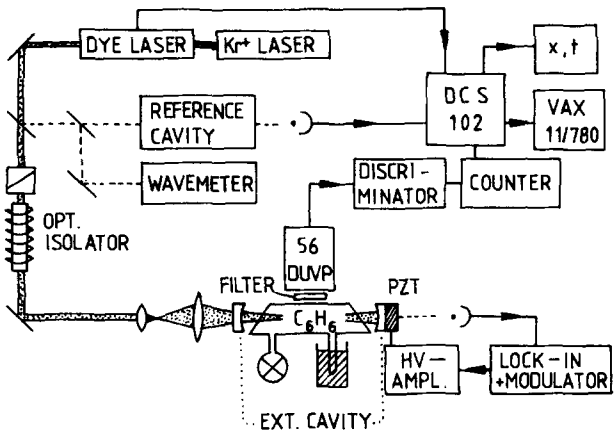

FIG. 1. Scheme of the experimental setup for homogeneous linewidth measurements by Doppler-free two-photon spectroscopy.

in an external concentric cavity as schematically shown in Fig. 1.[7] The signal enhancement made possible by an external cavity has been demonstrated previously for the measurement of two-photon Ramsey fringes[9] and pressure broadening and—shifts in rubidium.[8] With a piezo-mounted spherical end mirror ($r = 100$ mm) of 99% reflectivity and a spherical front mirror ($r = 100$ mm) of 70% reflectivity we measured a finesse of about 12. In order to lock the external cavity to the varying laser frequency, the mirror separation is slightly modulated. The resulting amplitude modulation of the transmitted light is fed into a phase-sensitive servo loop. With the external cavity the fluorescence signal produced by the Doppler-free two-photon absorption is larger by about a factor of 50 as compared to the standard setup and we are able to obtain accurate linewidth values at pressures as low as 0.5 Torr. The registration of the two-photon induced fluorescence and the data acquisition system is similar to that described in our previous work.[10]

III. EXPERIMENTAL RESULTS AND DISCUSSION

A. Linewidth as a function of vibrational excess energy

In Fig. 2 part of the blue edge of the Q branch of the $14_0^1 1_0^2$ two-photon band is shown as measured with linearly polarized light in the external cavity setup. In this band two quanta of the totally symmetric ν_1 vibration are excited in addition to one quantum of the two-photon inducing ν_{14} mode yielding a vibrational excess energy of 3412 cm^{-1} just above the onset of channel three. The benzene vapor pressure in this spectrum has been 0.5 Torr in order to suppress pressure broadening of the rotational lines. This part of the spectrum shows $K = 0$ lines with alternating intensities due to the different statistical weights for J even and J odd. All lines with $K \neq 0$ have disappeared as already published in our previous work,[5] however, for a higher pressure and lower spectral resolution. At the low pressure conditions of this work the background in the spectrum has completely disappeared and only the very sharp $K = 0$ lines are seen. Their peak intensity decreases with increasing J, the highest J is $J = 14$.

In addition to our previous spectrum another line is seen whose position coincides with the calculated $J_K = 0_0$ transition. The appearance of this line in the isotropic part of the totally symmetric vibronic band $14_0^1 1_0^2$ is in agreement with the well-known selection rules[11] and demonstrates the

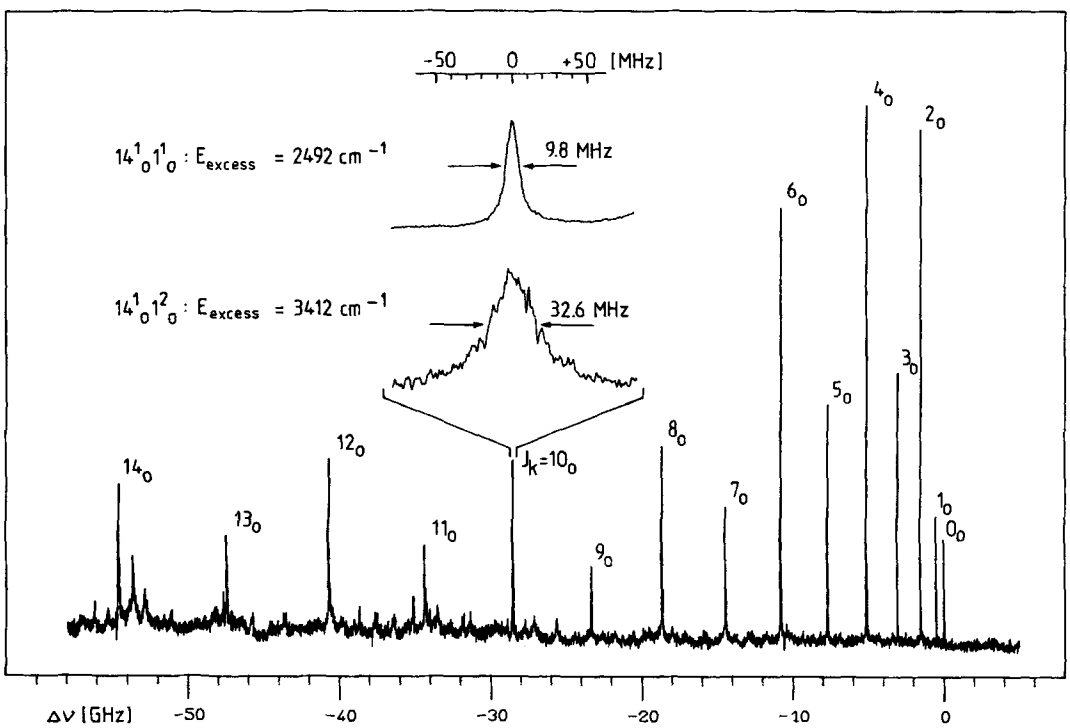

FIG. 2. Blue part of the Q branch of the $14_0^1 1_0^2$ two-photon band in C_6H_6 under Doppler-free high resolution. The $J_K = 10_0$ line is shown on an extended scale (lower trace of the inset). For comparison the same rotational line, however, in the $14_0^1 1_0^1$ band at lower vibrational excess energy is shown (upper trace of the inset). (Note that the scale is magnified by a factor as large as 100).

high resolution and sensitivity of our experimental setup. In the lower trace of the inset in Fig. 2 as an example the $J_K = 10_0$ line is shown on an extended scale demonstrating the high resolution in our measured spectrum. The observed line is nearly Lorentzian with a linewidth (FWHM) of 32.6 MHz.

For comparison the same rotational line ($J_K = 10_0$) has been studied, however, within the $14_0^1 1_0^1$ band at the lower excess energy of 2492 cm^{-1} due to the excitation of only a single quantum of the totally symmetric ν_1 vibration. Recently, we have shown that in the $14_0^1 1_0^1$ band all rotational lines appear with normal intensities given by the statistical weights, the Placzek–Teller factors, and the Boltzmann factors.[5,12] Obviously at the low excess energy of the $14_0^1 1_0^1$ band the rotationally dependent nonradiative process is not active. The result of our high resolution measurement is given in the upper trace of the inset. The observed line is found to be much sharper with a width (FWHM) of only 9.8 MHz. As will be shown below in this case the linewidth is mainly given by the residual pressure broadening and the experimental resolution of our apparatus. Therefore, the collisionless linewidth is expected to be about 2 MHz and hence smaller by a factor of 15 than the corresponding line in the $14_0^1 1_0^2$ band (lower trace). Comparison of the upper and the lower trace in the inset spectrum demonstrates the influence of vibrational excess energy on the linewidth of transitions for fixed rotational quantum numbers. We observe a 15-fold increase of collisionless linewidth when adding 920 cm^{-1} excess energy. Adding one further quantum of ν_1 ($14_0^1 1_0^3$) produces further broadening, so that our high resolution measurements do not reveal a line structure at all as we have shown recently.[5] The broadening at this high excess energy is so strong that individual lines are no longer resolved. This is in qualitative agreement with recent results from supersonic jet experiments[4]: Due to the low temperature, only few rotational transitions within the Q branch of the $14_0^1 1_0^3$ band appear whose integrated linewidth was found to be 37 GHz. Obviously, at this high energy level the nonradiative process has become so fast that any specific information can no longer be obtained.

B. Red part of the Q branch in the $14_0^1 1_0^2$ band: $J = K$ lines

In Fig. 3(b) as a second part of the spectrum the red part of the Q branch of the $14_0^1 1_0^2$ band is shown, starting 100 GHz away from the rotational origin of the vibronic band. This part of the band has been measured under the somewhat higher pressure of 4 Torr in order to increase the signal strength. In this part of the band also most of the lines have disappeared as can be seen from a comparison with Fig. 3(c) where the spectrum is shown as calculated from the appropriate rotational constants,[5] the statistical weights, Placzek–Teller, and Boltzmann factors. If the fluorescence quantum yield were constant for all rotational levels two-photon excitation measurements would yield the spectrum shown in Fig. 3(c). Indeed this spectrum with slightly changed relative positions is observed for the $14_0^1 1_0^1$ band where no rotationally selective nonradiative process is active.[5] A qualitative analysis reveals that the center of the remaining lines is better described by the position of $J = K$ lines rather than by that of $K = 0$ lines. This is demonstrated by the calculated positions for transitions with $J = K$ marked at the top of the spectrum.

At this point the origin of the anomalous structure need to be discussed. In recent work we have explained the disappearance of $K \neq 0$ lines for low J levels (blue edge of the Q branch in Fig. 2) by a Coriolis coupling produced by rotation R_z around the figure (z) axis of the benzene molecule (parallel Coriolis coupling). For the coupling strength of this type of Coriolis coupling induced by rotation R_z it has been found[13]

$$V_{Rz} \sim K \text{ with } \Delta K = 0. \tag{1}$$

Similarly, for Coriolis coupling induced by rotation R_x, R_y around the x and y axes (perpendicular Coriolis coupling) it is found

$$V^{+}_{R_{x,y}} \sim [(J-K)(J+K+1)]^{1/2} \text{ with } \Delta K = +1 \tag{2a}$$

and

$$V^{-}_{R_{x,y}} \sim [(J+K)(J-K+1)]^{1/2} \text{ with } \Delta K = -1. \tag{2b}$$

From Eqs. (1) and (2) it is clear that $K = 0$ lines are not affected by parallel Coriolis coupling whereas $J = K$ lines with $K \gg 1$ are not influenced by perpendicular Coriolis coupling. Hence the remaining $K = 0$ lines in the blue part of the spectrum (Fig. 2) are explained by R_z-Coriolis coupling whereas the $J = K$ structure in the red part of the spectrum points to a perpendicular ($R_{x,y}$) Coriolis coupling. This has been checked in more detail. The line intensities in the spectrum of Fig. 3(c) have been multiplied with the function

$$f(K,J) = [(J+K)(J-K+1) + (J-K)(J+K+1)]^{-1}, \tag{3}$$

which takes into account the typical dependence of the nonradiative process on K and J in the statistical limit and for perpendicular Coriolis coupling. The resulting spectrum is shown in Fig. 3(a). Surprisingly good agreement is found between the gross features in the calculated spectrum [Fig. 3(a)] and the measured spectrum in Fig. 3(b). This is another strong argument for Coriolis coupling to be responsible for the anomalous changes in the rotational structure of the $14_0^1 1_0^2$ band.

As a summary of the high resolution spectroscopic results shown in Fig. 2 for the blue part and in Fig. 3 for the red part of the Q branch it is concluded that in the two regions of the vibronic band two different types of Coriolis coupling are dominating. Up to final rotational state excess energies of 42 cm^{-1}, which correspond to -60 GHz in the Q-branch spectrum, parallel (R_z) Coriolis coupling is dominating, leaving $K = 0$ unaffected. For rotational state excess energies in S_1 between 70 and 195 cm^{-1} (-100 to -280 GHz in the Q branch) perpendicular ($R_{x,y}$) Coriolis coupling is strong, leaving $J = K$ lines unchanged. It is unlikely that there is a sharp stepwise onset of both types of Coriolis coupling in the two spectral regions under investigation. We may therefore expect that perpendicular Coriolis coupling is also existent in the low rotational excess energy range although much weaker and vice versa parallel Coriolis coupling is present in the red part of the Q branch in the high rotational excess energy range. This is in line with our recent

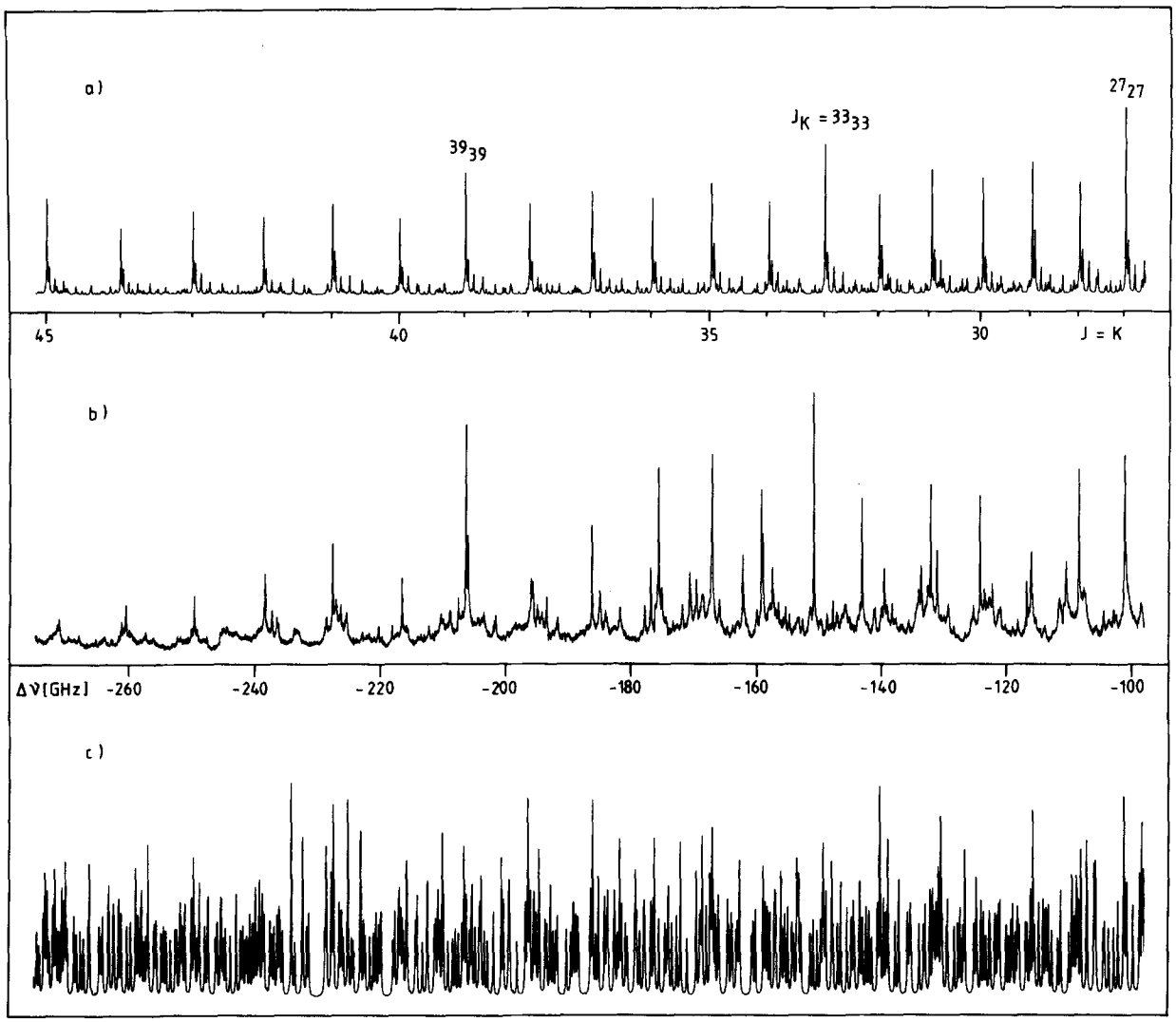

FIG. 3. Red part of the Q branch of the $14_0^1 1_0^2$ two-photon band under high resolution. (a) Calculated spectrum assuming a rotationally dependent fluorescence quantum yield according to Eq. (3). (b) measured spectrum; (c) spectrum calculated for a rotationally independent fluorescence quantum yield.

experimental result[6] demonstrating that there is a decrease of $K = 0$ line intensities with increasing J. It was explained by the additional perpendicular ($R_{x,y}$) Coriolis coupling since the line intensity of $K = 0$ lines shows the typical $[J(J+1)]^{-1}$ dependence expected from Eq. (2) for a statistical model. On the other hand in Fig. 3(b) it is seen that the $J = K$ lines begin to die out for increasing K, probably due to weak parallel (R_z) Coriolis coupling also present in this energy range. This type of Coriolis coupling increases with K according to Eq. (1) and leads to a decrease of the fluorescence quantum yield.

Here, it has been assumed that Coriolis coupling is the primary process of a subsequent intramolecular vibrational relaxation and a final electronic relaxation process that does not depend on rotational quantum numbers.[6]

In order to corroborate the underlying assumptions it is important to investigate whether the line shape of the $K = 0$ lines also changes with increasing J. While the intensity in the excitation spectra of Figs. 2 and 3 which represents relative fluorescence quantum yield measurements is sensitive only to an electronic relaxation process, line shapes also contain information about vibrational relaxation mechanisms within S_1. In this way additional quantitative information about coupling and level mixing within S_1 is obtained and elucidation of the nature of the nonradiative process and the coupling mechanism is expected.

C. Collisional and transient time broadening

In order to obtain accurate linewidth values the measured linewidths have to be corrected for residual pressure broadening still present for pressures below 1 Torr. Another contribution is due to the spectral resolution of our experimental set up mainly given by the transient time broadening within the small focus of the laser beam.[14]

Both contributions, collisional broadening as well as instrumental resolution, can be corrected for from the results shown in Fig. 4. Here the typical pressure dependence of the linewidth is shown for the rotational line $J_K = 12_0$ in the $14_0^1 1_0^1$ band (□) and the $14_0^1 1_0^2$ band (○). This pressure dependence has been also checked for other rotational lines within the $14_0^1 1_0^2$ band as well as in the $14_0^1 1_0^1$ band yielding

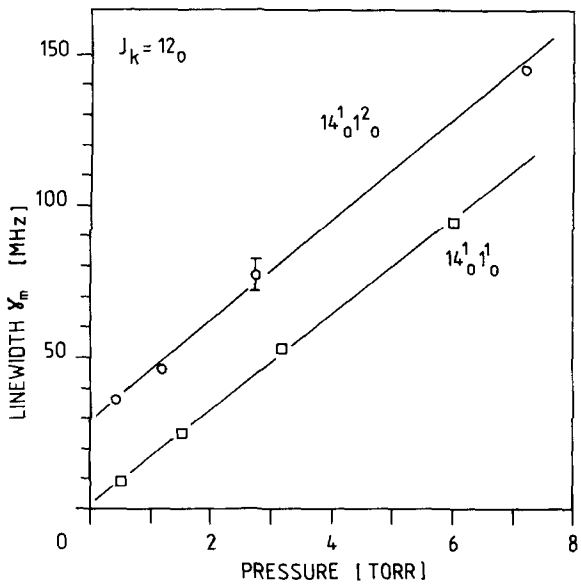

FIG. 4. Linewidth γ_m of the rotational line $J_K = 12_0$ measured as a function of C_6H_6 pressure in the range between 0.5 and 8 Torr. Upper points (○) represent measured linewidth values of the $J_K = 12_0$ line in the $14^1_0 1^2_0$ band, lower points (□) measured values for the same rotational line, however, in the $14^1_0 1^1_0$ band at lower excess energy. Solid lines represent the best fit to the experimental points. All points represent average values. The error bar indicates the largest observed error.

similar slopes of about 15 MHz/Torr for the different rotational lines. Hence a good value for the collisional line broadening parameter γ_{coll} in the vibronic band $14^1_0 1^2_0$ is 15 MHz/Torr and it is clear that reliable collision-free linewidths are only obtained for pressures below 0.5 Torr. From the collisional line broadening parameter γ_{coll} the collisional rate is calculated and a value of $K_{coll} = 2\pi\gamma_{coll} = 9.4\times 10^7$ s^{-1} Torr^{-1} is found. This value exceeds even the largest value for K_{coll} found from fluorescence quantum yield and lifetime measurements[15] and from intensities of emission bands in dispersed fluorescence[16] by a factor of 3. The disagreement is reasonably well explained by the fundamental difference of the experimental techniques used in Refs. 15 and 16 and in this work. In our case also elastic collisions with a larger cross section are expected to contribute to the collision linewidth γ_{coll} leading to a larger collisional frequency than in Refs. 15 and 16, where due to the different experimental technique, only energy changing collisions in the excited state have been investigated. It is, however, important that the Doppler-free homogeneous linewidth measurements of this work for the first time yield precise values for state selective collisional rates of electronically excited polyatomic molecules.

The instrumental resolution of the experimental setup is found from the pressure dependence of the much narrower $J_K = 12_0$ line in the $14^1_0 1^1_0$ progression. The solid line represents the pressure dependence of the linewidth and is extrapolated to zero pressure. From Fig. 4 the extrapolated collisionless linewidth of the $J_K = 12_0$ line in the $14^1_0 1^1_0$ band is found to be about 2 MHz. This is in agreement with our recent low resolution lifetime measurements of this band[17] from which a value of $\tau = 70$ ns has been found. Since in the Doppler-free high resolution spectrum of this band no rotationally dependent nonradiative process has been observed we may take this broadband value as a good estimate for the collisionless linewidth of the particular rotational line $J_K = 12_0$ under consideration. Taking into account that the rovibronic ground state is extremely sharp, we obtain from $\gamma = 1/2\pi\tau$ a value of $\gamma = 2.3$ MHz close to the value of 2 MHz extrapolated from the pressure dependence in Fig. 4. Therefore, its contribution to the measured linewidths is small and the line shape measured at the lowest pressure of 0.5 Torr enables us to obtain a reliable value for the instrumental resolution of our experimental setup. The line shapes obtained for narrow lines with less than 15 MHz linewidth resemble Voigt profiles, i.e., a convolution of a near Gaussian line due to the transient time broadening and the laser linewidth of 1 MHz and a Lorentzian line due to the homogeneous broadening [for comparison see upper line in the inset of Fig. 2 and Fig. 5(a)]. A deconvolution of both the near Gaussian contribution and the Lorentzian contribution yeilds an instrumental resolution of 5 MHz. We have compared this value with recent work on transient time broadening in which a similar two-photon set up has been used and found good agreement of our value with the value due to transient time broadening in the foci of the counterpropagating laser beams and the laser linewidth.[14]

The observed line shape $A(\omega - \omega_0)$ is given by a convolution of the Lorentzian collisionless line $L_{rel}(\omega - \omega_0)$, the Lorentzian residual collisional broadening $L_{coll}(\omega - \omega_0)$, and the Gaussian instrumental line $G(\omega - \omega_0)$, i.e.,

$$A(\omega - \omega_0) = G(\omega - \omega_0) \otimes \{L_{coll}(\omega - \omega_0) \otimes L_{rel}(\omega - \omega_0)\}.$$

To obtain the width of the homogeneous line the Gaussian contribution was first removed by a computer deconvolu-

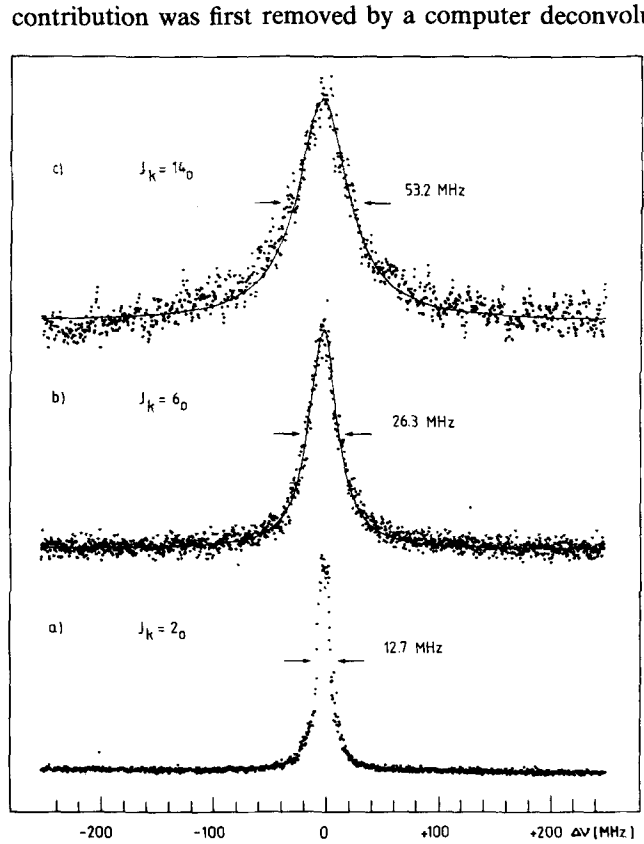

FIG. 5. Measured line shapes for three different single rotational lines in the $14^1_0 1^2_0$ two-photon band of C_6H_6. (a) $J_K = 2_0$, (b) $J_K = 6_0$, (c) $J_K = 14_0$. Solid lines represent the Lorentzian line shapes fitted to the experimental points.

tion. Subtraction of the known collisional linewidth of 15 MHz/Torr from the resulting Lorentzian linewidth yields the linewidth of the collisionless line profile.

D. Linewidth dependence on rotational quantum number

Linewidths have been measured for all $K = 0$ lines at the blue edge of the Q branch (see Fig. 1) from $J = 0$ up to $J = 14$. In this part of the spectrum mainly $K = 0$ lines appear so that the assignment is unambiguous. Three typical measured line shapes are shown in Fig. 5 for (a) $J_K = 2_0$, (b) $J_K = 6_0$, (c) $J_K = 14_0$. The benzene vapor pressure in this measurement was 0.44 Torr and all lines in Fig. 5 are normalized to constant height. It is seen that the linewidth for the three rotational lines with different J is completely different. The measured linewidth increases by a factor of 4 from 12.7 MHz (a) to 53.2 MHz (c). From above we know that there is a constant near Gaussian contribution to the linewidth of 5 MHz from instrumental resolution and a constant Lorentzian contribution of 6.6 MHz from collisional broadening at a pressure of 0.44 Torr. In Table I all measured linewidths γ_m (FWHM) for the $K = 0$ lines with different J are listed together with the deconvoluted collisionless relaxation linewidths γ and the corresponding relaxation rate $K = 2\pi\gamma$. These linewidths are produced by the intramolecular relaxation process. The smallest collisionless relaxation linewidth is found to be 1.3 MHz for the $J_K = 0_0$ transition. Within the error limit this value is close to the collisionless linewidth of the rotational lines in the $14_0^1 1_0^1$ band at the lower excess energy of 2492 cm^{-1}. Γ is found to increase smoothly with increasing J up to 46.1 MHz. This is a 30-fold increase in the observed range from $J = 0$ up to $J = 14$. This result points to a radiationless relaxation process which is strongly dependent on the rotational quantum number J and increases strongly with J within a single vibrational band, i.e., for constant vibrational excess energy.

IV. DISCUSSION

The information obtained from the experimental results in the previous section can be summarized as follows:

TABLE I. Measured linewidths γ_m, deconvoluted collisionless relaxation linewidths γ and corresponding relaxation rates $K = 2\pi\gamma$ for the observed rotational transitions with $K = 0$ and different J values. Values are accurate to about $\pm$ 5%.

$J,K=0$	γ_m[MHz]	γ[MHz]	$K \times 10^{-6}$[s^{-1}]
0	10.4	1.3	8.2
1	10.9	1.9	11.9
2	12.7	4.0	25.1
3	15.1	6.8	42.7
4	17.6	9.5	59.7
5	20.7	12.8	80.4
6	26.3	18.7	118
7	29.6	22.1	139
8	32.8	25.4	160
9	34.8	27.4	172
10	32.6	25.2	158
11	33.4	26.0	163
12	37.1	29.8	187
13	36.3	29.0	182
14	53.2	46.1	290

(i) Up to rotational excess energies of 42 cm^{-1} in the $14^1 1^2$ state (blue edge of the Q branch) only lines with $K = 0$ are observed; (ii) the line shape of the lines with $J > 6$ measured under nearly collision-free conditions is Lorentzian to a high accuracy; (iii) collisionless relaxation linewidth γ increases from 1.3 MHz for $J_K = 0_0$ to 46.1 MHz for $J_K = 14_0$.

From these experimental results several conclusions may be drawn. Since Fig. 2 represents a fluorescence excitation spectrum it is obvious that the fluorescence from all lines with $K \neq 0$ has disappeared due to a rapid nonradiative electronic relaxation process. This nonradiative process is weaker by several orders of magnitude for the remaining $K = 0$ lines but increases rapidly with J as can be seen from the decreasing intensity of the $K = 0$ lines with increasing J.[6] It is hard to understand that electronic relaxation in benzene can so strongly depend on molecular rotation.[18] Therefore, it is expected that the observed strong dependence on rotation of the molecule is produced by a primary intramolecular vibrational relaxation process (IVR) within S_1. Linewidths then are determined by the intramolecular vibrational relaxation process (IVR) rather than by the nonradiative electronic relaxation process. In the past IVR processes have been studied for a series of organic molecules[19] mainly by the method of collisional timing of fluorescence spectra. The question of the coupling mechanism responsible for the IVR process, i.e., the level mixing within the S_1 vibrational manifold is still open. In our previous work we concluded on the basis of our high resolution results that second-order Coriolis coupling is responsible for coupling of the optically excited modes to the background modes in S_1 of benzene. More recently a similar result has been found by Forch *et al.*[20] for the pyrimidine molecule with intermediate level structure.

Similarly, the results in Fig. 2 and Fig. 3 of this work plead for Coriolis coupling as the responsible coupling mechanism. The part of the spectrum shown in Fig. 2 with the remaining $K = 0$ lines has already been interpreted in our recent work[5] as due to strong parallel Coriolis coupling (R_z) produced by rotation around the z axis. The remaining $J = K$ lines in the spectrum of Fig. 3 are thought to be the result of strong perpendicular Coriolis coupling ($R_{x,y}$) around the x and y axes which mainly affects lines with $K < J$ as shown in Eq. (2). The decreasing intensity and increasing linewidth of the $K = 0$ lines is explained by an additional but weaker perpendicular ($R_{x,y}$) Coriolis coupling present in the region with strong parallel (R_z) Coriolis coupling since the perpendicular Coriolis coupling matrix element is known to increase with $[J(J+1)]^{1/2}$. Thus $K = 0$ lines with larger J are stronger coupled to background states by perpendicular Coriolis coupling. The dependence has been investigated in our recent work[6] and there has been found reasonable agreement with the typical $J(J+1)$ dependence of perpendicular Coriolis coupling.

Now it has to be discussed whether the additional information about the increase of collisionless linewidth is in line with Coriolis coupling as the dominating coupling mechanism. Since the observed line shapes are Lorentzian to a high accuracy obviously the Coriolis coupling mechanism leads to an irreversible relaxation process. Such a relaxation is present in the statistical limit, i.e., if $\rho \gg V^{-1}$ where ρ is the

density of background states which are coupled to the optically excited state by Coriolis coupling and V is the coupling matrix element which represents the strength of the coupling process. The order of magnitude of the Coriolis coupling strength V for benzene can be estimated from the well known case of parallel Coriolis coupling between the two components of a degenerate vibration, e.g., the ν_6 vibration with $\xi_z = 0.6$. One obtains $V_z \sim \xi_z CK \approx 0.055\ K\ \mathrm{cm}^{-1}$. Correspondingly for the case of perpendicular Coriolis coupling

$$V^{\pm} \sim \xi_{x,y} B\,[(J \mp K)(J \pm K + 1)]^{1/2}.$$

For $K = 0$ lines only perpendicular Coriolis coupling is active. For $K = 0$ and $\xi_{x,y} \approx 1$ we obtain

$$V^{\pm} \sim \xi_{x,y} B\,[J(J+1)]^{1/2} \approx 0.2[J(J+1)]^{1/2}\mathrm{cm}^{-1}.$$

Then typically as an upper limit we obtain, e.g., $V^{\pm} \lesssim 0.28\ \mathrm{cm}^{-1}$ for $J = 1$ and $V^{\pm} \lesssim 2.9\ \mathrm{cm}^{-1}$ for $J = 14$.

In the statistical limit the relaxation rate K is given by

$$K \approx V^2 \rho \tag{4}$$

and therefore $\gamma \sim J(J+1)$ for $K = 0$ if ρ does not depend itself on J.

In order to check this dependence in Fig. 6 the experimentally found relaxation linewidth γ of the $K = 0$ lines is plotted as a function of $J(J+1)$. Up to $J = 9$ reasonable agreement with the theoretically expected linear dependence on $J(J+1)$ is obtained. However, for higher J the observed increase of linewidth is not as pronounced as expected from the increase of coupling strength according to Eq. (4). An explanation for the deviation might be a decrease of the density ρ of suitable background states in this energy range giving rise to a smaller relaxation rate $K = 2\pi\gamma$.

Finally, it has to be discussed whether the density ρ of coupled states in the case of Coriolis coupling is sufficient to fulfill the conditions for the statistical limit $\rho \gg V^{-1}$. For the estimated coupling strengths of about 1 cm^{-1} it is hard to understand how the density of states condition should be fulfilled, particularly if one bears in mind that there exist not only $\Delta K, \Delta J$ (rotational) but also strict Δv (vibrational) selection rules for second order Coriolis coupling.[13]

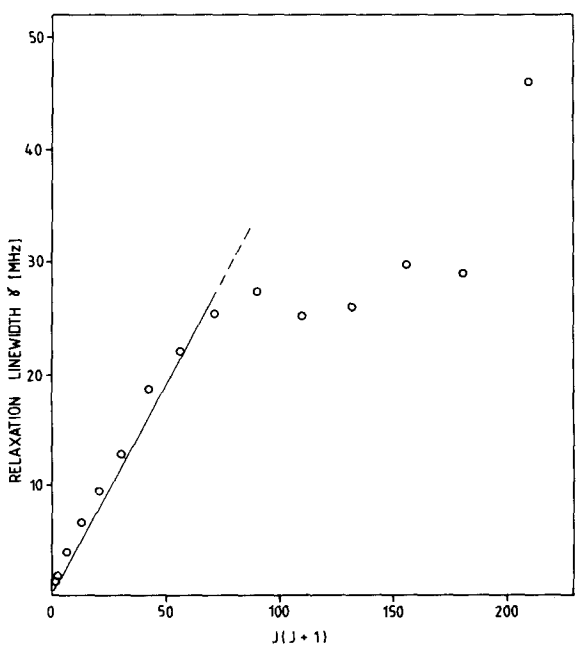

FIG. 6. Experimental results for intramolecular relaxation linewidths γ of several lines with $K = 0$ from $J = 0$ up to $J = 14$ as a function of $J(J+1)$. Solid line represents a linear fit to the first experimental points.

At first sight it is difficult to realize that Coriolis coupling could increase the level densities of the vibronic manifold by adding the rotational level manifold if J and K are good quantum numbers and conserved during the coupling process. An explanation would be that higher order Coriolis coupling increases effective background level densities. This would, however, decrease the coupling strength. In this case the $\Delta K = \pm 1$ selection rules of the perpendicular Coriolis coupling could lead to a K mixing with an increase of effective density of coupled levels as has been discussed for vibrational levels of high excess energy in S_0.[21]

Callomon[22] has suggested the alternative explanation that electronic coupling to an intermediate still unknown electronic state occurs which then itself is coupled into the quasicontinuum of S_0.

Another promising model seems to us a two-step coupling scheme. Coriolis coupling represents the first coupling step to a quasicontinuum produced by only a few background states. The irreversibility of the coupling process is then guaranteed by a second coupling step which couples the intermediate background state to a dense manifold of states and broadens the background states. This second coupling step possibly represents strong anharmonic coupling or more likely fast electronic relaxation processes. Several processes have been discussed as responsible for the strong decrease of fluorescence quantum yield in C_6H_6, e.g., internal conversion (IC) and isomerization. It may be concluded from recent results of Otis *et al.*[23] that ISC is not the relevant relaxation mechanism in the channel three region. For a coupling of two states (one of them broadened) the relaxation rate $K = 2\pi\gamma$ of the optically excited state can be concluded from a two-state model as, e.g., presented in Ref. 24:

$$K \sim V_{\alpha}^{2-i}, \tag{5}$$

where α is the linewidth of the broadened background state. Also in this case the relaxation rate K and the collisionless linewidth γ depend on V^2 and reveal the typical dependence on $J(J+1)$ which has been studied in Fig. 6.

V. SUMMARY AND CONCLUSION

In this work for the first time the Doppler-free homogeneous linewidth has been measured for rovibronic transitions of a polyatomic molecule at room temperature. These measurements have been performed in order to obtain information about the intramolecular nonradiative relaxation process. Inhomogeneous Doppler broadening in the benzene (C_6H_6) gas phase spectrum was eliminated by the technique of Doppler-free two-photon spectroscopy. The spectral resolution of 5 MHz in our experiment is mainly given by transient time broadening in the small focus of the two counterpropagating laser beams. Hence, reliable collisionless linewidths have been available for measured linewidths exceeding 10 MHz.

We have investigated the $14_0^1 1_0^2$ vibronic band with a

vibrational excess energy of 3412 cm^{-1} in S_1. From conventional Doppler-limited absorption spectra as well as from fluorescence quantum yield measurements it has previously been concluded that there is the onset of a new radiationless process (channel three) around 3000 cm^{-1}. It is therefore of particular interest to measure Doppler-free rotationally resolved (single rotational line) spectra in this excess energy range. In our recent Doppler-free experiment we found anomalous results in the $14_0^1 1_0^2$ band: Nearly all rotational lines have disappeared in the spectrum and solely $K = 0$ lines for $J \leqslant 14$ are still present in the spectrum. From this we concluded that the nonradiative process in this excess energy range is strongly dependent on the rotational quantum numbers of the molecules.

In this work additional information about the nonradiative process is obtained from the measurement of collisionless linewidths of the previously detected $K = 0$ lines from $J = 0$ up to $J = 14$.

From the experimental results in this work it is unambiguous that Coriolis coupling gives rise to the abovementioned observed phenomena and plays an important role in nonradiative relaxation processes in this range of the benzene spectrum. Therefore, we conclude that Coriolis coupling is a primary process responsible for the channel three nonradiative process in this excess energy range. There remain however, several open questions concerning the magnitude of the coupling strength. More severely, it is difficult to explain the high density of background states necessary for the irreversible relaxation process observed in our experiment in view of the rotational as well as the vibrational selection rules present for second order Coriolis coupling. It will be necessary to discuss more sophisticated models including K mixing and higher order Coriolis coupling.

In conclusion it has been shown that Doppler-free two-photon spectroscopy is a valuable technique for the study of intramolecular nonradiative relaxation processes in polyatomic molecules. It has been demonstrated that it is inevitable to resolve single rotational lines even for polyatomic molecules since nonradiative relaxation linewidth is shown to change by nearly two orders of magnitude for neighboring lines within a single vibronic band differing only slightly in J and K.

It is shown in this work that the understanding of the nature of the coupling mechanism stems from the observation of rotational levels with $J \gg 1$. These states are not observed in cooled jet experiments but are amenable in Doppler-free two-photon spectra in room temperature bulk gas presented in this work.

In particular, collisionless homogeneous linewidths represent a valuable source of information on intramolecular nonradiative processes which is complementary to that obtained from fluorescence decay measurements within the time domain.

ACKNOWLEDGMENTS

The authors are indebted to Professor Dr. E. W. Schlag for his permanent interest in this work. They thank H. Stepp for his help in performing the experiments. Financial support from the Deutsche Forschungsgemeinschaft is greatfully acknowledged.

[1](a) For a review see: C. S. Parmenter, Adv. Chem. Phys. **22**, 365 (1972); (b) L. Wunsch, H. J. Neusser, and E. W. Schlag, Z. Naturforsch. Teil A **36**, 1340 (1981).
[2]J. H. Callomon, J. E. Parkin, and R. Lopez-Delgado, Chem. Phys. Lett. **13**, 125 (1972).
[3]J. H. Callomon, T. M. Dunn, and I. M. Mills, Phil. Trans. R. Soc. London Ser. A **259**, 99 (1965).
[4]K. Aron, C. Otis, R. E. Demaray, and P. M. Johnson, J. Chem. Phys. **73**, 4167 (1980).
[5]E. Riedle, H. J. Neusser, and E. W. Schlag, J. Phys. Chem. **86**, 4847 (1982).
[6]E. Riedle, H. J. Neusser, E. W. Schlag, and S. H. Lin, J. Phys. Chem. (in press).
[7]E. Riedle, H. Stepp, H. J. Neusser, in *Laser Spectroscopy VI*, edited by H. P. Weber and W. Lüthy (Springer, Berlin, 1983), p. 144.
[8]Wan-Ü. L. Brillet and A. Gallagher, Phys. Rev. A **22**, 1012 (1980).
[9]S. A. Lee, J. Helmcke, and J. L. Hall, in *Laser Spectroscopy IV, Springer Series in Optical Sciences*, edited by H. Walther and K. W. Rothe (Springer, Berlin, 1979), Vol. 21, p. 130.
[10]E. Riedle, H. J. Neusser, and E. W. Schlag, J. Chem. Phys. **75**, 4231 (1981).
[11]G. Placzek, Rayleigh-Streuung, and Ramaneffekt, in *Handbuch der Radiologie Bd.* 6, edited by E. Marx (Akademische Verlagsqesellschaft, Leipzig, 1934).
[12]E. Riedle, R. Moder, and H. J. Neusser, Opt. Commun. **43**, 388 (1982).
[13]I. M. Mills, Pure Appl. Chem. **11**, 325 (1965).
[14]F. Biraben, M. Bassini, and B. Cagnac, J. Phys. (Paris) **40**, 445 (1979).
[15]K. G. Spears and S. A. Rice, J. Chem. Phys. **55**, 5561 (1971).
[16]C. S. Parmenter, B. Setzer, and K. Y. Tang, J. Chem. Phys. **66**, 1317 (1977).
[17]L. Wunsch, H. J. Neusser, and E. W. Schlag, Chem. Phys. Lett. **32**, 210 (1975).
[18]F. A. Novak and S. A. Rice, J. Chem. Phys. **73**, 858 (1980).
[19]C. S. Parmenter, J. Phys. Chem. **86**, 1735 (1982), and references cited therein.
[20]B. E. Forch, K. T. Chen, H. Saigusa, and E. C. Lim, J. Phys. Chem. **87**, 2280 (1983).
[21]H. L. Dai, E. Abramson, R. W. Field, D. Imre, J. L. Kinsey, C. L. Korpa, D. E. Reisner, and P. H. Vaccaro, in *Laser Spectroscopy VI*, edited by H. P. Weber and W. Lüthy (Springer, Berlin, 1983), p. 74.
[22]J. H. Callomon, Discuss Faraday Soc. General Discuss. Nr. (to be published).
[23]C. E. Otis, J. L. Knee, P. M. Johnson, J. Phys. Chem. **87**, 2232 (1983).
[24]A. Nitzan, J. Jortner, J. Kommandeur, and E. Drent, Chem. Phys. Lett. **9**, 273 (1971).